INTERNATIONAL JOURNAL OF HYDROGEN ENERGY 37 (2012) 6109–6117

Available online at www.sciencedirect.com

SciVerse ScienceDirect

journal homepage: www.elsevier.com/locate/he

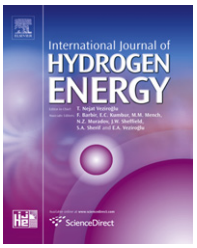

MOF-5 composites exhibiting improved thermal conductivity

D. Liu [a,b], J.J. Purewal [a,b], J. Yang [a,*], A. Sudik [a], S. Maurer [c], U. Mueller [c], J. Ni [b], D.J. Siegel [b,*]

[a] Ford Motor Company, Research and Advanced Engineering, MD 1170/RIC, Dearborn, MI 48121, USA

[b] Mechanical Engineering Department, University of Michigan, 2350 Hayward St., Ann Arbor, MI 48109, USA

[c] BASF SE, Chemicals Research and Engineering, 67056 Ludwigshafen, Germany

ARTICLE INFO

Article history:
Received 13 September 2011
Received in revised form
21 December 2011
Accepted 22 December 2011
Available online 20 January 2012

Keywords:
Hydrogen storage materials
Metal-organic frameworks
MOF-5
Thermal conductivity
Surface area

ABSTRACT

The low thermal conductivity of the prototype hydrogen storage adsorbent, metal-organic framework 5 (MOF-5), can limit performance in applications requiring rapid gas uptake and release, such as in hydrogen storage for fuel cell vehicles. As a means to improve thermal conductivity, we have synthesized MOF-5-based composites containing 1–10 wt.% of expanded natural graphite (ENG) and evaluated their properties. Cylindrical pellets of neat MOF-5 and MOF-5/ENG composites with densities of 0.3, 0.5, and 0.7 g/cm^3 are prepared and assessed with regard to thermal conductivity, specific heat capacity, surface area, and crystallinity. For pellets of density ~0.5 g/cm^3, we find that ENG additions of 10 wt.% result in a factor of five improvement in thermal conductivity relative to neat MOF-5, increasing from 0.10 to 0.56 W/mK at room temperature. Based on the relatively higher densities, surface areas, and enhanced crystallinity exhibited by the composites, ENG additions appear to partially protect MOF-5 crystallites from plastic deformation and/or amorphization during mechanical compaction; this suggests that thermal conductivity can be improved while maintaining the favorable hydrogen storage properties of this material.

1. Introduction

Metal-organic framework 5 (MOF-5) is a microporous, crystalline solid comprised of 1,4-benzenedicarboxylate (BDC) organic linkers and Zn_4O tetrahedral clusters that serve as secondary building units [1,2]. The high-surface area and permanent porosity of MOF-5 make it an attractive material for a variety of applications [3], including: catalysis [4,5], gas storage [6–10], gas separation [11,12], gas purification [13], and sensing [14].

Regarding gas storage, MOF-5 has been extensively studied for automotive hydrogen storage applications [1,7–10,15,16]. This interest stems from the observation that MOF-5 can adsorb a large amount of hydrogen, up to 7.1 excess wt.% at 77 K and 40 bar [15], via an exothermic reaction with a heat of adsorption ranging from 2 to 5 kJ/mol·H_2 [17]. In order to achieve targeted refueling times – the 2017 U.S. Dept. of Energy Target is 3.3 min for 5 kg H_2 [18] – and maximize the amount of hydrogen stored, it is desirable to remove the heat generated during adsorption from the storage bed in order to quickly reach the desired operating temperature (e.g., 77 K).

With conventional synthesis methods, MOF-5 is obtained as a loose powder consisting of small cubic crystallites (<1 μm) with low bulk density (ρ = 0.13 g/cm^3) [19]. As powder morphologies are typically not conducive to efficient thermal transport, the thermal conductivity of MOF-5 powders is expected to be less than the single-crystal value of 0.32 W/mK (T = 300 K) [16,20,21]. Owing to their large pore sizes (e.g., >20 Å diameter) and high free volumes (e.g., >90%) [22], the thermal conductivity of many microporous materials (e.g.,

* *Corresponding authors.*
E-mail addresses: jyang27@ford.com (J. Yang), djsiege@umich.edu (D.J. Siegel).
0360-3199/$ – see front matter
doi:10.1016/j.ijhydene.2011.12.129

zeolites and MOFs) is low [22–25]. As pointed out in Ref. [21], the atomic number density, which correlates with thermal conductivity, can be lower in MOFs (2.46×10^{28} atoms/m^3 for MOF-5) than in zeolites (5.13×10^{28} atoms/m^3 for sodalite) [26], suggesting that MOFs may exhibit extremes of thermal conductivity behavior, even in comparison to other microporous materials.

Consistent with the low atomic and bulk densities of MOF-5, our preliminary measurements on low-density MOF-5 pellets found a thermal conductivity of less than 0.08 W m^{-1} K^{-1} ($T = 45$ °C) [16]. This low conductivity can place limitations on the design of MOF-5-based storage systems. For example, a low thermal conductivity can hinder fast refueling for adsorption processes which rely on a pressure or temperature-swing. Although engineering approaches aimed at mitigating these limitations are possible, all common strategies involve tradeoffs in efficiency or the density of stored hydrogen. (For example, a heat-exchanging manifold could be incorporated within the storage vessel. However, the extra space and mass associated with this device will lower the volumetric and gravimetric density of the system [27].) Thus, the identification of methods to improve the thermal conductivity of the hydrogen storage material would minimize the need for auxiliary thermal components, and result in improved system performance. These methods could also be applicable to other microporous materials such as MOFs, zeolites, and the broader class of framework materials [e.g., zeolitic imidizolate frameworks (ZIFs) and covalent organic frameworks (COFs)].

In a previous study we reported the effect of powder densification on several properties of neat MOF-5, such as excess and total hydrogen storage capacity, surface area, pore volume, crystallinity, and crush strength [16]. By determining these processing–structure–property relationships, we revealed tradeoffs associated with densifying MOF-5 for on-board hydrogen storage applications. For example, we found that a nearly 400% improvement in the excess volumetric H_2 capacity could be achieved through compaction [e.g., increasing from 7 g H_2/L at $\rho = 0.13$ g/cm^3 (powder) to 26 g H_2/L for $\rho = 0.51$ g/cm^3 (pellet) at 77 K and 70 bar]. However, these improvements came at the cost of a small decrease in excess gravimetric capacity (−15% at $\rho = 0.51$ g/cm^3) and limited improvement in thermal conductivity (increasing from less than 0.08 W/mK to 0.16 W/mK at 26 °C as pellet density increased from 0.35 to 0.69 g/cm^3). To our knowledge, studies aimed at improving the thermal conductivity of MOFs have not been reported, and we are aware of only two reports of thermal conductivity characterization of MOFs in the literature [20,21]. Both of these studies focused on assessing the thermal conductivity for a single crystal of MOF-5.

Toward the goal of improving the thermal conductivity of MOF-5-based hydrogen storage materials, here we investigate the effect of forming composites of MOF-5 with varying additions of expanded natural graphite (ENG) worms (i.e., natural graphite soaked in sulfuric acid and heated to high temperatures [28,29]). Given its high thermal conductivity (~150 W/mK [29]), and the fact that carbons are also known to act as hydrogen adsorbents [30], the addition of ENG to MOF-5 compacts presents a potentially promising method for improving thermal conductivity while maintaining favorable hydrogen storage properties. Small quantities of ENG have been successfully used as thermal conductivity enhancers for a variety of metal and complex hydride storage materials such as $NaAlH_4$ [27], La–Ni–Sn [28,29], MgH_2 [31], $LaNi_5$ [32], and $Mg_{90}Ni_{10}$ [33]. For example, the thermal conductivity of MgH_2 at 300 K was increased from 0.7 W/mK (neat MgH_2) to 7.5 W/mK with the addition of 10 wt.% ENG [31]. In this study we systematically examine the impacts of varying ENG content and compact density on the thermal conductivity, surface area, specific heat capacity, and crystallinity of densified MOF-5/ENG composites. For ~0.5 g/cm^3 pellets we find that ENG additions of 10 wt.% result in a factor of five improvement in thermal conductivity relative to neat MOF-5, increasing from 0.10 to 0.56 W/mK at 298 K. In addition, we observe that composites having less than or equal to 10 wt.% ENG largely preserve the crystallinity and high-surface area of MOF-5; this suggests that thermal conductivity can be improved while maintaining the favorable hydrogen storage properties of this material.

2. Experimental details

Powder samples of MOF-5 were prepared and desolvated as previously described in Refs. [16,19]; ENG worms were used as purchased (SGL Group). Compacts were prepared with three bulk densities of approximately 0.3, 0.5 and 0.7 g/cm^3. MOF-5 was mixed with ENG using a Spex 8000 mixer/mill with ENG contents of 1, 5, and 10 wt.% for 20 s. The post-mixed MOF-5/ENG blends were loaded into cylindrical punches and dies with different bore diameters, i.e., 6.35 mm (for specific heat capacity and surface area measurements) and 12 mm (for thermal diffusivity and XRD measurements). Specimens were compressed using a manual pellet press (Reflex Analytical, which was housed inside the glovebox) for 6.35 mm pellets, and a 12 ton hydraulic press (Carver, 4350 manual pellet press) for 12 mm pellets. This latter bench-top press was located outside of the glovebox. To minimize exposure of MOF-5 to humid air, dry nitrogen gas was blown across the die set during pressing. By applying different press forces, pellets of different bulk densities were obtained. Bulk densities were calculated from the mass and physical dimensions of each pellet. The resulting pellets are cylindrical with flat ends, as shown in Fig. 1.

The thermal conductivities λ of all pellets were calculated at 26, 35, 45, 55 and 65 °C using the following equation:

$$\lambda = \alpha \cdot C_p \cdot \rho \quad (1)$$

where α is the thermal diffusivity, ρ is the compact density and C_p is the specific heat capacity. Specific heat capacity measurements were performed on the 6.35 mm pellets with a differential scanning calorimeter (DSC) (SENSYS DSC, Setaram), which was calibrated with a sapphire standard. Pellets were placed inside an alumina crucible inside the glovebox and then transferred to the DSC (external to the glovebox). Data were collected using a heating rate of 5 °C/min and a He carrier gas flow of 20 ml/s. Thermal diffusivity measurements were performed with a xenon thermal flash diffusivity instrument (Anter Flashline, FL3000S2) using N_2 as

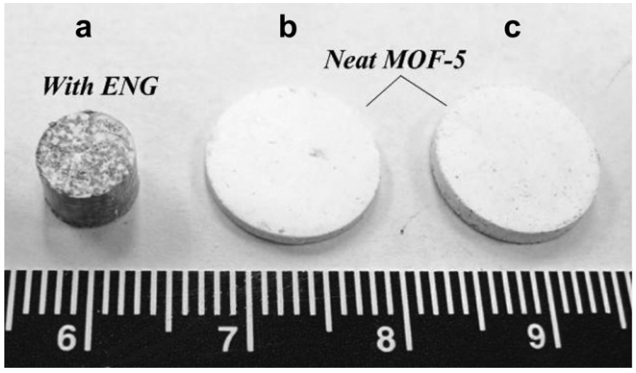

Fig. 1 – Cylindrical pellets of neat MOF-5 and MOF-5/ENG composites. (a) Pellet of 6.35 mm diameter and 4.9 mm thickness for specific heat capacity measurements and surface area measurements. (b) Pellet of 12 mm diameter and 1 mm thickness for XRD measurements, and (c) pellet of 12 mm diameter and 2 mm thickness for thermal diffusivity measurements.

protective gas, based on pellets with 12 mm diameter and 2 mm average thickness. The instrument was calibrated using an iron standard. A thin layer of silver paint was applied to the top surfaces to prevent the pellets from fracturing during measurement, and the lower surfaces of the pellets were coated with graphite to improve light absorption. Before measuring, the pellets were first evacuated at room temperature for at least 2 h and then heated at 130 °C under vacuum for at least 3 h.

Surface area measurements were performed by nitrogen adsorption at 77 K with a Micromeritics ASAP 2010 with average sample sizes of 400 mg. Surface area values were calculated according to the Langmuir (or BET) equations. Powder X-ray Diffraction (PXRD) data were collected on a SCINTAG (XDS2) powder diffractometer operated at 45 kV and 40 mA with step increments of 0.02° and a rate of 2 s/step using Cu Kα radiation (λ = 1.5418 Å). Samples used for PXRD were loaded in the glovebox and maintained under a N_2 atmosphere during data collection. Scanning electron microscopy (SEM) was used to examine the microstructure of MOF-5 and ENG at an accelerating voltage of 15 kV and a working distance of 39 mm on a JEOL 840A SEM. Prior to SEM imaging, the MOF-5 was coated with a thin carbon layer to make its surface electrically conducting in the SEM using a Denton Carbon Coater.

3. Results and discussion

3.1. Microstructure

Optical and SEM images of MOF-5 and as purchased ENG worms are shown in Fig. 2(a) and (b), respectively. The MOF-5 powder is composed of particles of cubic morphology with individual crystallite sizes of less than 1 μm, and interparticle voids of several microns in diameter. The particle size distribution and topology of interparticle voids in the neat MOF-5 compact can affect several important engineering properties, such as bulk density, permeation of gases, thermal conductivity, and total surface area. In particular, the submicron particle size of MOF-5 can impact its packing density, lead to an increased contribution of external surface area (and consequently interparticle porosity within the pellet), and negatively impact permeability and particle strength [34]. Fig. 2(b) shows the SEM images for the as purchased ENG

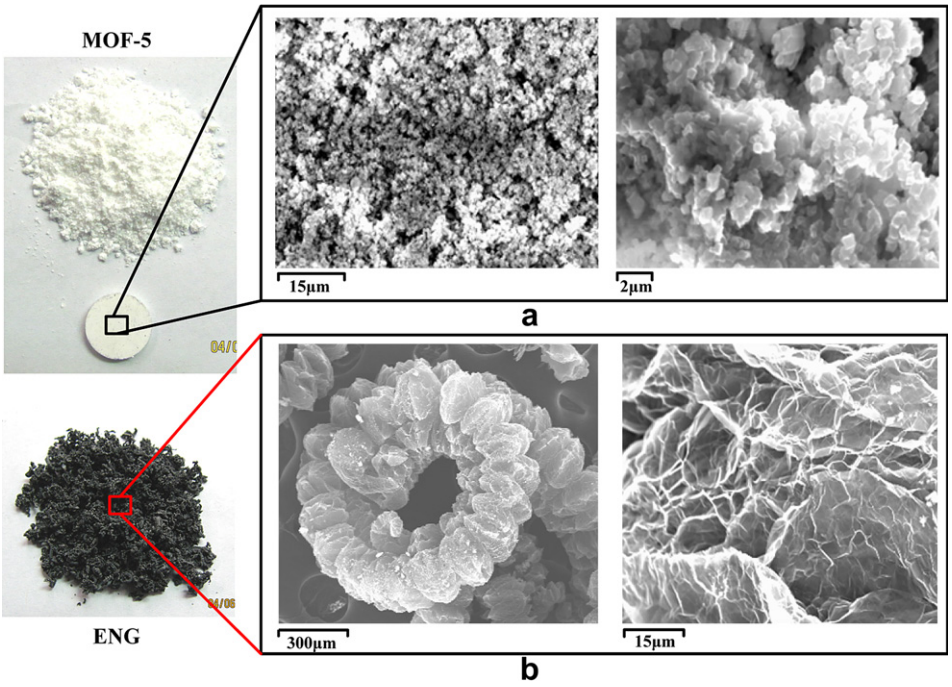

Fig. 2 – Optical (left) and SEM (right) microstructure images of (a) MOF-5 (powder and pellet of 0.49 g/cm^3) and (b) as purchased ENG.

worms, which were prepared from natural graphite. By applying heat treatment, the lamella structure of natural graphite can be transformed into a vermicular "worm" structure through expansion and exfoliation as shown in Fig. 2(b). The ENG powder is composed of vermicular particles of 0.1 to several millimeters in size. In addition, the ENG maintains the high thermal conductivity (~150 W/mK [29]) of the original expandable graphite, since it possesses the same in-plane super-lattice ordering [32].

3.2. *Pellet density and applied pressure*

Fig. 3 illustrates the relationship between pellet density and applied pressure over an explored pressure range of 8–315 MPa. This relationship is essentially independent of ENG content. For pressures less than 150 MPa the pellet density increases in roughly a linear fashion. Beyond 150 MPa, the density approaches a limiting value of approximately 1.7 g/cm^3, a value nearly three times that of the single-crystal density (0.61 g/cm^3). Although neat MOF compacts and MOF/ENG compacts share the same functional relationship between density and pressure (e.g., linear below 150 MPa), the magnified inset in Fig. 3 suggests that increased ENG additions consistently result in slightly higher densities in the low-pressure regime. This implies that ENG is more easily compressed relative to MOF-5, and we speculate that deformation may be localized within the ENG during the early stages of compaction (at low pressures). Consequently the presence of ENG could prove beneficial during the compaction process by absorbing the initial load and acting as a lubricant to distribute mechanical energy. As the applied pressure becomes greater, the ENG will approach its compression limit and further load increases will be borne by MOF-5.

3.3. *Crystallinity*

Powder X-ray diffraction (PXRD) data was obtained in order to evaluate MOF-5 structural stability/crystallinity during the compacting process both in presence and absence of ENG. Fig. 4 compares PXRD patterns of neat MOF-5 and MOF-5/10 wt.% ENG for densities of approximately 0.5 and 0.7 g/cm^3. For the MOF-5 specimens containing ENG (Fig. 4(c) and (d)), a high intensity diffraction peak corresponding to graphite (2θ = 26.5°) is observed, with no other notable changes in the XRD patterns. This suggests that no significant structural changes occur in the composites upon addition of ENG compared to the neat MOF-5 compacts with comparable density. Increasing compact density, however, does result in decreased intensity of MOF-5 diffraction peaks for specimens with identical dimensions (i.e. exposed diameter and thickness). For example, for the neat MOF-5 compacts, the intensity of the main diffraction peak (2θ = 6.9°) decreases by 50% in going from 0.49 g/cm^3 to 0.67 g/cm^3 (Fig. 4(a) and (b)). On the other hand, for pellets with 10 wt.% ENG the diffraction intensity decreases by only 38% upon a similar increase in density (Fig. 4(c) and (d)). The lower decrease in peak intensity for the composite pellets (with ENG) supports the hypothesis that ENG additions could aid in the protection of MOF-5 crystallites from plastic deformation/amorphization during mechanical compaction, as previously discussed.

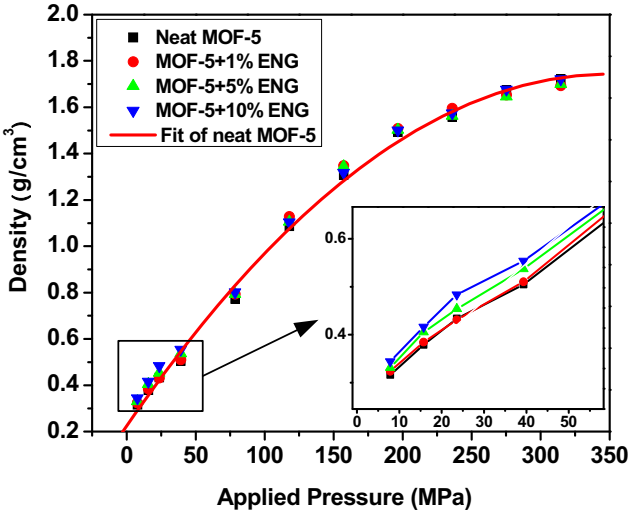

Fig. 3 – Pellet density verses applied pressure for MOF-5 with different contents of ENG.

It has been reported that the MOF-5 crystal structure will transform to an amorphous phase at the relatively low applied pressure of 3.5 MPa [35]. However, in this study, and consistent with our previous findings for neat MOF-5 [16], for the pellet density of 0.7 g/cm^3 a considerable fraction of the crystalline phase persists as shown in Fig. 4(b) and (d). Based on the calibration curve in Fig. 3, a density of 0.7 g/cm^3 corresponds to an applied pressure of around 64 MPa. This difference in behavior could potentially be attributed to the different synthesis and desolvation methods used in the prior study [35]. Nevertheless, the consistent decrease in diffraction peak intensity coupled with the increase in diffuse scattering does indicate a progressive transformation from crystalline to amorphous. Similarly, the peak intensity of ENG is also decreased with increasing density.

3.4. *Surface area and hydrogen adsorption*

It is well established that the amount of hydrogen adsorbed per unit mass (i.e. excess gravimetric capacity) in typical high-surface area adsorbents is proportional to the sorbent's specific surface area [36–38]. It is preferable that improvements to the thermal conductivity of MOF-5 via ENG additions and/or densification do not come at the expense of degrading other important properties. The effect of ENG content and compact density on the BET surface area, total N_2 adsorption volume and monolayer capacity Q_m of MOF-5 are summarized in Table 1.

Prior studies on neat MOF-5 and MOF-177 have revealed that powder compaction reduces surface area [16,39]. In the case of MOF-5, forming a compact with density of 0.3 g/cm^3 reduces the BET surface area by 1.7% as compared to the neat powder; increasing the pellet density further to ~0.5 g/cm^3 results in a larger decrease of 18%. The trends for total N_2 adsorption volume and monolayer capacity Q_m are similar with increasing density. This effect is expected to arise from the collapse of intraparticle voids (micro porosity) of MOF-5 due to amorphization and/or plastic deformation [39].

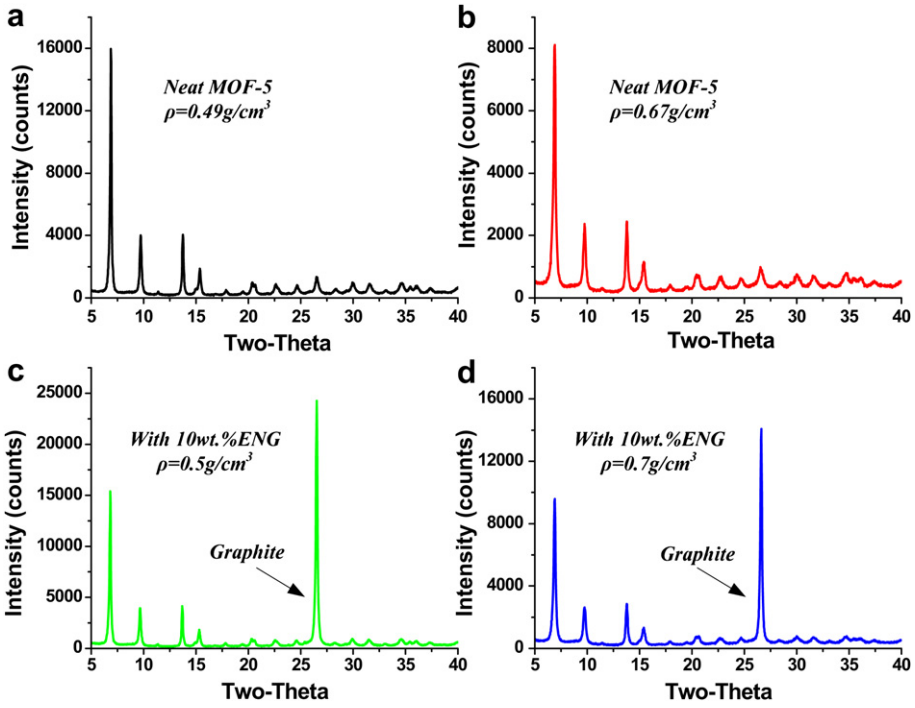

Fig. 4 – XRD patterns of pellets of neat MOF-5 with densities of (a) 0.49 g/cm^3 and (b) 0.67 g/cm^3, and of MOF-5 with 10 wt.% ENG composites with densities of (c) 0.5 g/cm^3 and (d) 0.7 g/cm^3.

Although the surface area of ENG (20 m^2/g [40]) is more than two orders of magnitude smaller than that of MOF-5, the BET surface area, total N_2 adsorption volume and monolayer capacity Q_m of MOF-5/ENG compacts do not exhibit significant decreases relative to the neat MOF-5 compacts of comparable density. On the contrary, a slight increase on the BET surface area and Q_m of the lower density MOF-5/ENG compacts (i.e. 0.3 & 0.5 g/cm^3) is observed comparing with neat MOF-5 compacts. For example, in contrast to the neat pellets, MOF-5/5 wt.%-ENG composite pellets at ~0.3 and ~0.5 g/cm^3 exhibit a slight increase and smaller decrease (5%) in BET surface area, respectively, relative to the neat powder. For total N_2 adsorption volume, there is a general decreasing trend with adding ENG, especially with larger amounts added (e.g., 10 wt.%), which indicates the added ENG may have influence H_2 adsorption.

As discussed previously, the presence of ENG may "protect" the MOF during compression. However, this protective effect appears to cease when density/compacting pressure becomes larger (e.g., 0.7 g/cm^3). At this density the pellets having higher ENG content exhibit lower surface areas relative to the neat MOF-5 pellet. An additional trend that emerges from the data is that for a given density the surface areas of the MOF-5/ENG composite pellets exhibit decreasing surface areas as their ENG content increases, as expected from the lower surface area of ENG. In summary, at moderate densities (up to 0.5 g/cm^3) and concentrations (up to 5 wt.%) ENG additions to MOF-5 do not significantly degrade those properties that are correlated with surface area.

Table 1 – Effect of ENG content and compact density on the BET surface area, total N_2 adsorption volume, and monolayer capacity Q_m of MOF-5.

Sample	BET SA (m^2/g)	Tot. N_2 Ad. Vol. (cm^3/g)	Q_m (cm^3/g STP)
Powder (Neat) $\rho = 0.3$ g/cm^3	2763	1.36	635
Neat	2715	1.34	624
1 wt.% ENG	2927	1.27	672
5 wt.% ENG	2781	1.21	639
10 wt.% ENG	2665	1.17	612
$\rho = 0.5$ g/cm^3			
Neat	2263	1.12	520
1 wt.% ENG	2584	1.12	594
5 wt.% ENG	2623	1.14	603
10 wt.% ENG	2413	1.06	554
$\rho = 0.7$ g/cm^3			
Neat	1999	0.87	459
1 wt.% ENG	2022	0.88	464
5 wt.% ENG	1888	0.82	434
10 wt.% ENG	1760	0.77	404

Table 2 – Hydrogen adsorption at 77 K by the MOF-5/ENG pellets with 0 wt.% and 10 wt.% ENG.

Description	Density (g/cm^3)	Max H_2 adsorption at 77 K (wt.%)
Powder MOF-5	0.13	5.64
0 wt.% ENG	0.31	5.76
	0.51	4.72
	0.603	4.17
10 wt.% ENG	0.324	4.75
	0.479	4.21
	0.716	3.49

Table 2 lists the maximum hydrogen excess adsorption at 77 K by the MOF-5/ENG pellets with 0 wt.% and 10 wt.% ENG. A more detailed study of the hydrogen storage performance for MOF-5/ENG compacts will be the subject of a future publication. Table 1 and Table 2 show that the trend of max H_2 uptake is mostly consistent with that of surface area. However there are some exceptions to the general trend. For example, the 10 wt.% ENG ($\rho = 0.5$ g/cm^3) has a larger surface area than the 0 wt.% ENG ($\rho = 0.5$ g/cm^3), but the max H_2 uptake is lower. In general, the MOF-5/ENG pellets have a lower maximum adsorption of H_2 at 77 K compared to the neat MOF-5 pellets for the same density, consistent with the total N_2 adsorption volume (from 1.12 cm^3/g for MOF-5 to 1.06 cm^3/g for MOF-5/10 wt.%-ENG). This result indicates that for microporous materials such as MOFs, the total volume of gas adsorbed in each composite is a better measure of gas capacity.

3.5. *Specific heat capacity*

The specific heat capacity (C_p) is a thermodynamic property that describes to the ability of a material to store thermal energy. In particular, the heat capacity dictates the amount of energy one must put into the system in order to heat the material to a certain temperature. Heat capacity can be an important property for gas storage systems relying on temperature-swing operation. The heat capacity of pellets of neat MOF-5 and MOF-5/ENG composites at temperatures of 26, 35, 35, 55 and 65 °C were measured and are plotted in Fig. 5.

The specific heat capacities increase with increasing temperature for all the samples examined. The value of C_p at 26 °C for MOF-5 with density of 0.3 g/cm^3 is 0.73 J/g °C, and is comparable to that of graphite (0.71 J/g °C) [41]. For a fixed density, the specific heat capacity increases with increasing ENG concentration. For example, at the density of 0.5 g/cm^3 the heat capacity for the MOF-5 compact with 10 wt.% ENG increases by almost 6% at 26 °C (from 0.73 to 0.77 J/g °C) and almost 10% at 65 °C (from 0.85 to 0.93 J/g °C) relative to neat MOF-5 compact. However, as shown in Fig. 5(d), the C_p of neat ENG is comparable to that of neat MOF-5, suggesting that the C_p of the MOF-5/ENG blends should not be altered relative to the neat MOF-5 compacts. A possible explanation for the observed increase in C_p with increasing ENG additions may be traced to ENG's ability to preserve the crystallinity of MOF-5 during the compaction process (as discussed above). In support of this hypothesis we note that for a fixed ENG content C_p decreases with increasing compact density; presumably this is due to a decrease in MOF-5 crystallinity.

3.6. *Thermal conductivity*

The thermal conductivity for compacts of MOF-5 and MOF-5/ENG composites were calculated based on Eq. (1) at 26, 35, 45, 55 and 65 °C, and as a function of pellet density (see Fig. 6). In total, measurements on 60 distinct samples were performed. The neat MOF-5 pellets exhibit very low thermal conductivities independent of density. For example, a thermal

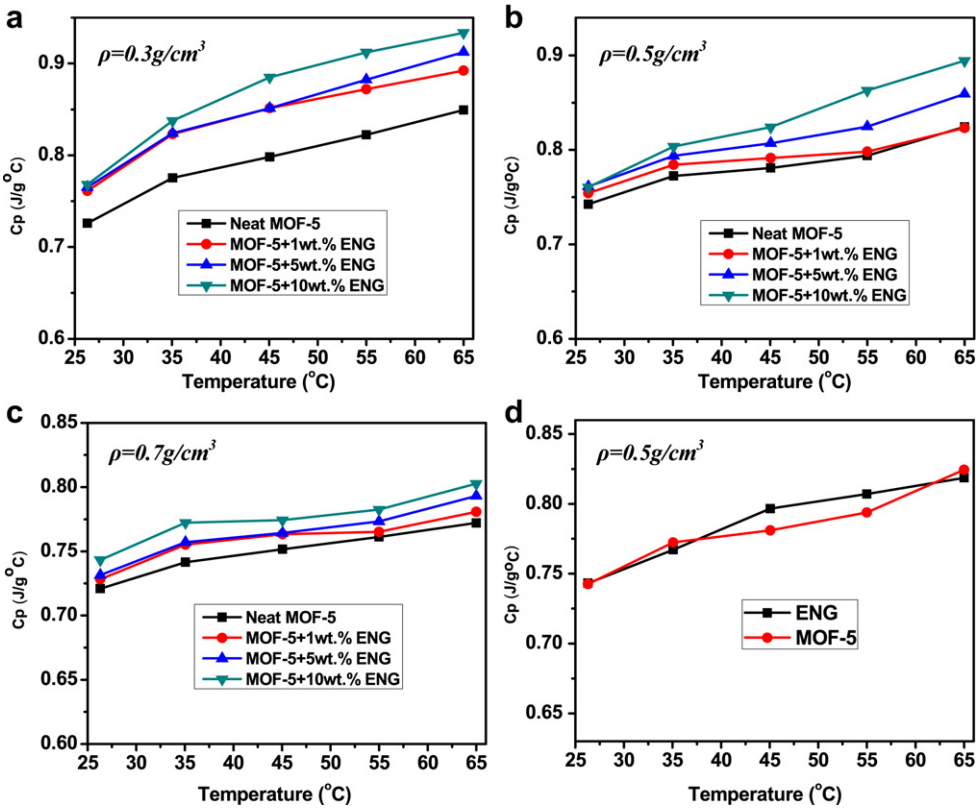

Fig. 5 – Specific heat capacity of pellets of neat MOF-5 and MOF-5/ENG composites as a function of density, ENG content, and temperature. (a)–(c) Pellets with densities of 0.3, 0.5, and, 0.7 g/cm^3, respectively; (d) comparison of neat MOF-5 pellets with neat ENG pellets, both with density of 0.5 g/cm^3.

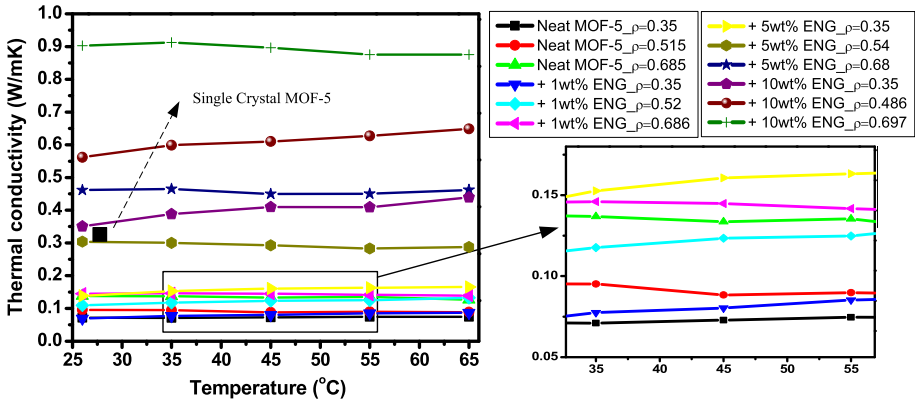

Fig. 6 – Thermal conductivity of pellets of neat MOF-5 and MOF-5/ENG composites as a function of density, ENG content, and temperature (T = 26–65 °C).

conductivity of 0.10 W/mK is observed for the 0.5 g/cm^3 neat MOF-5 compact at 26 °C, which is approximately one third of the conductivity value for the single crystal (0.32 W/mK [20,21]). Adding 1 wt.% ENG has little effect on the thermal conductivity (e.g., it increases to 0.11 W/mK for a density of 0.52 g/cm^3 at 26 °C). On the other hand, increasing the ENG content to 5 or 10 wt.% resulted in a significant enhancement in thermal conductivity. In particular, the thermal conductivity at 26 °C for the 0.5 g/cm^3 compact increases by factors of three and five upon addition of 5 wt.% and 10 wt.% ENG (0.30 and 0.56 W/mK), respectively, as compared with neat MOF-5. Notably, these pellets exhibit conductivities that approximately equal (5 wt.% ENG) or nearly double (10 wt.% ENG) the values obtained for single crystal MOF-5 [20,21].

The thermal conductivities of the composite pellets show only a weak temperature dependence over the narrow temperature range examined. This is consistent with single crystal [20,21] and neat MOF-5 pellet data [16] taken at the same temperatures. Future studies will probe the temperature dependence of thermal conductivity at the cryogenic temperatures (77 K) needed for significant uptake of hydrogen gas.

Increasing pellet density also results in an increase in the thermal conductivity. For example, the thermal conductivity for a neat MOF-5 compact doubles (from 0.07 to 0.14 W/mK at 26 °C) as density is increased from 0.3 to 0.7 g/cm^3 [3,16]. Under similar conditions, a greater enhancement of more than 2.5 times was achieved (from 0.35 to 0.90 W/mK) for composite pellets containing 10 wt.% ENG. Increasing pellet density appears to enhance the conductivity by decreasing the amount of interparticle void space within the pellet. The relatively larger increases in thermal conductivity observed in the presence of ENG may be attributed to improvements in the extent and nature of the interfacial contact between MOF-5 and ENG particles.

Taken together, Fig. 4 and Table 1 indicate that for densities up to 0.5 g/cm^3 the addition of up to 10 wt.% ENG helps to preserve the crystallinity and surface area of MOF-5-based composites. ENG additions also improve the thermal conductivity noticeably (Fig. 6). Based on Fig. 6, if the amount of added ENG is less than 5 wt.%, there is no significant improvement on the thermal conductivity. Hence, the optimal range for ENG additions appears to lie within 5–10 wt.%; this should result in a significant improvement in thermal conductivity without large decreases to other hydrogen storage properties.

4. Conclusions

Densified MOF-5 composites containing expanded natural graphite (ENG) were explored as a means to improve the low thermal conductivity of MOF-5 powders. MOF-5 was mixed with 1, 5, or 10 wt.% ENG and compressed into cylindrical pellets with densities of 0.3, 0.5, and 0.7 g/cm^3. The thermal conductivity, specific heat capacity, surface area, and crystallinity of the resulting MOF-5/ENG composites were evaluated and compared to neat MOF-5 compacts of the same density. The key findings of this study can be summarized as follows:

1) Based on the higher densities and enhanced crystallinity exhibited by MOF-5/ENG composites, ENG additions appear to partially protect MOF-5 crystallites from plastic deformation and/or amorphization during mechanical compaction. We speculate that ENG may preferentially absorb a portion of the compressive load and act as a lubricant to distribute mechanical energy.
2) Prior studies for neat MOF-5 revealed that compaction reduces surface area. Despite the small surface area of ENG, at moderate pellet densities (up to 0.5 g/cm^3) and ENG concentrations (up to 5 wt.%), ENG additions to MOF-5 do not significantly degrade those properties (such as hydrogen storage capacity) that are correlated with surface area.
3) Small ENG additions (~1 wt.%) yield less than a 10% improvement in thermal conductivity compared to neat MOF-5 pellets of the same density. However, larger additions of 5 and 10 wt.% yield significant improvements of 3 and 5 times, respectively (~0.5 g/cm^3). Increasing the pellet density also improves the thermal conductivity: Compacting pellets from 0.3 to 0.7 g/cm^3 improves the thermal conductivity by 2 (neat MOF-5) and 2.5 times (MOF-5/10 wt.% ENG), respectively.

Taken together, the impact of ENG additions on thermal conductivity, surface area, and crystallinity suggests that optimal properties are obtained for ENG additions of 5–10 wt.% and pellet densities of ~0.5 g/cm^3. As the present study focuses on thermal conductivity in the axial direction at near-ambient temperatures, future work will target lower temperatures (i.e. 10–298 K), conductivity in the radial direction, and alternative thermal conductivity enhancers (e.g. Al). We expect that the results of this study will prove beneficial for further improving of the thermal conductivity of MOF-5 and other MOFs, and can also be used to aid in the design of efficient MOF-5-based storage systems.

Acknowledgments

The authors acknowledge Drs. Andy Drews and James Boileau at Ford for help with the XRD and SEM measurements, and Giovanni Cavataio and Jim Warner for the surface area analyses. Funding for this study was provided by the U.S. Department of Energy, Office of Energy Efficiency and Renewable Energy, grant no. DE-FC36-GO19002.

REFERENCES

[1] Li H, Eddaoudi M, O'Keeffe M, Yaghi OM. Design and synthesis of an exceptionally stable and highly porous metal-organic framework. Nature 1999;402:276–9.
[2] James SL. Metal-organic frameworks. Chemical Society Reviews 2003;32:276–88.
[3] Meek ST, Greathouse JA, Allendorf MD. Metal-organic frameworks: a rapidly growing class of versatile nanoporous materials. Advanced Materials 2011;23:249–67.
[4] Opelt S, Türk S, Dietzsch E, Henschel A, Kaskel S, Klemm E. Preparation of palladium supported on MOF-5 and its use as hydrogenation catalyst. Catalysis Communications 2008;9:1286–90.
[5] Zhao N, Deng HP, Shu MH. Preparation and catalytic performance of Pd catalyst supported on MOF-5. Chinese Journal of Inorganic Chemistry 2010;26:1213–7.
[6] Saha D, Bao Z, Jia F, Deng S. Adsorption of CO_2, CH_4, N_2O, and N_2 on MOF-5, MOF-177, and zeolite 5A. Environmental Science and Technology 2010;44:1820–6.
[7] Yang J, Sudik A, Wolverton C, Siegel DJ. High capacity hydrogen storage materials: attributes for automotive applications and techniques for materials discovery. Chemical Society Reviews 2010;39:656–75.
[8] Li J, Cheng S, Zhao Q, Long P, Dong J. Synthesis and hydrogen-storage behavior of metal-organic framework MOF-5. International Journal of Hydrogen Energy 2009;34:1377–82.
[9] Saha D, Deng S, Yang Z. Hydrogen adsorption on metal-organic framework (MOF-5) synthesized by DMF approach. Journal of Porous Materials 2009;16:141–9.
[10] Sillar K, Hofmann A, Sauer J. Ab initio study of hydrogen adsorption in MOF-5. Journal of the American Chemical Society 2009;131:4143–50.
[11] Gallo M, Glossman-Mitnik D. Fuel gas storage and separations by metal-organic frameworks: simulated adsorption isotherms for H_2 and CH_4 and their equimolar mixture. Journal of Physical Chemistry C 2009;113:6634–42.
[12] Keskin S, Sholl DS. Assessment of a metal-organic framework membrane for gas separations using atomically detailed calculations: CO_2, CH_4, N_2, H_2 Mixtures in MOF-5. Industrial & Engineering Chemistry Research 2008;48:914–22.
[13] Li JR, Kuppler RJ, Zhou HC. Selective gas adsorption and separation in metal-organic frameworks. Chemical Society Reviews 2009;38:1477–504.
[14] Halder GJ, Kepert CJ, Moubaraki B, Murray KS, Cashion JD. Guest-dependent spin crossover in a nanoporous molecular framework material. Science 2002;298:1762–5.
[15] Kaye SS, Dailly A, Yaghi OM, Long JR. Impact of Preparation and Handling on the hydrogen storage properties of Zn_4O(1,4-benzenedicarboxylate)3 (MOF-5). Journal of the American Chemical Society 2007;129:14176–7.
[16] Purewal JJ, Liu D, Yang J, Sudik A, Siegel DJ, Maurer S, Müler U. Increased volumetric hydrogen uptake of MOF-5 by powder densification. International Journal of Hydrogen Energy 2012;37:2723–7.
[17] Schmit B, Müller U, Trukhan N, Schubert M, Férey G, Hirscher M. Heat of adsorption for hydrogen in microporous high-surface-area materials. ChemPhysChem 2008;9:2181–4.
[18] http://www1.eere.energy.gov/hydrogenandfuelcells/storage/pdfs/targets_onboard_hydro_storage.pdf.
[19] Mueller U, Schubert M, Teich F, Puetter H, Schierle-Arndt K, Pastre J. Metal-organic frameworks-prospective industrial applications. Journal of Materials Chemistry 2006;16:626–36.
[20] Huang BL, McGaughey AJH, Kaviany M. Thermal conductivity of metal-organic framework 5 (MOF-5): Part I. Molecular dynamics simulations. International Journal of Heat and Mass Transfer 2007;50:393–404.
[21] Huang BL, Ni Z, Millward A, McGaughey AJH, Uher C, Kaviany M, et al. Thermal conductivity of a metal-organic framework (MOF-5): part II. Measurement. International Journal of Heat and Mass Transfer 2007;50:405–11.
[22] McGaughey AJH, Kaviany M. Thermal conductivity decomposition and analysis using molecular dynamics simulations part II. Complex silica structures. International Journal of Heat and Mass Transfer 2004;47:1799–816.
[23] Griesinger A, Spindler K, Hahne E. Measurements and theoretical modelling of the effective thermal conductivity of zeolites. International Journal of Heat and Mass Transfer 1999;42:4363–74.
[24] Greenstein A, Hudiono Y, Graham S, Nair S. Effects of nonframework metal cations and phonon scattering mechanisms on the thermal transport properties of polycrystalline zeolite LTA films. Journal of Applied Physics 2010;107. Art. No. 063518.
[25] Murashov VV, White MA. Thermal properties of zeolites: effective thermal conductivity of dehydrated powdered zeolite 4A. Materials Chemistry and Physics 2002;75:178–80.
[26] Wyckoff RWG. Crystal structures. 2 ed. New York: John Wiley and Sons, Interscience; 1963.
[27] http://www.hydrogen.energy.gov/pdfs/review11/st006_van_hassel_2011_o.pdf.
[28] Klein HP, Groll M. Heat transfer characteristics of expanded graphite matrices in metal hydride beds. International Journal of Hydrogen Energy 2004;29:1503–11.
[29] Sánchez AR, Klein HP, Groll M. Expanded graphite as heat transfer matrix in metal hydride beds. International Journal of Hydrogen Energy 2003;28:515–27.
[30] Ichikawa T, Chen DM, Isobe S, Gomibuchi E, Fujii H. Hydrogen storage properties on mechanically milled graphite. Materials Science and Engineering B: Solid-State Materials for Advanced Technology 2004;108:138–42.
[31] Chaise A, de Rango P, Marty P, Fruchart D, Miraglia S, Olivès R, et al. Enhancement of hydrogen sorption in magnesium hydride using expanded natural graphite. International Journal of Hydrogen Energy 2009;34:8589–96.
[32] Kim KJ, Montoya B, Razani A, Lee KH. Metal hydride compacts of improved thermal conductivity. International Journal of Hydrogen Energy 2001;26:609–13.

[33] Pohlmann C, Röntzsch L, Kalinichenka S, Hutsch T, Kieback B. Magnesium alloy-graphite composites with tailored heat conduction properties for hydrogen storage applications. International Journal of Hydrogen Energy 2010; 35:12829–36.
[34] German RM. Particle packing characteristics. Princeton, NJ: Metal Powder Industries Federation; 1989.
[35] Hu YH, Zhang L. Amorphization of metal-organic framework MOF-5 at unusually low applied pressure. Physical Review B – Condensed Matter and Materials Physics 2010;81. Art. No. 174103.
[36] Murray LJ, Dinc M, Long JR. Hydrogen storage in metal-organic frameworks. Chemical Society Reviews 2009;38: 1294–314.
[37] Rowsell JLC, Yaghi OM. Strategies for hydrogen storage in metal-organic frameworks. Angewandte Chemie – International Edition 2005;44:4670–9.
[38] Béard P, Chahine R. Modeling of adsorption storage of hydrogen on activated carbons. International Journal of Hydrogen Energy 2001;26:849–55.
[39] Zacharia R, Cossement D, Lafi L, Chahine R. Volumetric hydrogen sorption capacity of monoliths prepared by mechanical densification of MOF-177. Journal of Materials Chemistry 2010;20:2145–51.
[40] http://www.matweb.com/search/datasheet.aspx?matguid=7b9f8d75083043288d1ca2b4a410d737.
[41] http://en.wikipedia.org/wiki/Heat_capacity#cite_note-hypph-20.